AGU PUBLICATIONS

JGR

Journal of Geophysical Research: Atmospheres

RESEARCH ARTICLE
10.1002/2015JD023546

**Key Points:**
- Upward propagation speed in PB stage decreases with its initiation altitude
- PB pulse characteristics are related with vertical speed and initiation altitude
- Step length of initial leader in PB stage increases with initiation altitude

**Correspondence to:**
T. Wu,
wu.ting@comf5.comm.eng.osaka-u.ac.jp

**Citation:**
Wu, T., S. Yoshida, Y. Akiyama, M. Stock, T. Ushio, and Z. Kawasaki (2015), Preliminary breakdown of intracloud lightning: Initiation altitude, propagation speed, pulse train characteristics, and step length estimation, *J. Geophys. Res. Atmos.*, *120*, 9071–9086, doi:10.1002/2015JD023546.

Received 20 APR 2015
Accepted 16 AUG 2015
Accepted article online 19 AUG 2015
Published online 17 SEP 2015
Corrected 4 DEC 2015

This article was corrected on 4 DEC 2015. See the end of the full text for details.



# Preliminary breakdown of intracloud lightning: Initiation altitude, propagation speed, pulse train characteristics, and step length estimation

**Ting Wu[1], Satoru Yoshida[2], Yasuhiro Akiyama[1], Michael Stock[1,3], Tomoo Ushio[1], and Zen Kawasaki[1,3]**

[1]Division of Electrical, Electronic and Information Engineering, Graduate School of Engineering, Osaka University, Osaka, Japan, [2]Meteorological Research Institute, Ibaraki, Japan, [3]RAIRAN Pte. Ltd., Osaka, Japan

**Abstract** Using a low-frequency lightning location system comprising 11 sites, we located preliminary breakdown (PB) processes in 662 intracloud (IC) lightning flashes during the summer of 2013 in Osaka area of Japan. On the basis of three-dimensional location results, we studied initiation altitude and upward propagation speed of PB processes. PB in most IC flashes has an initiation altitude that ranges from 5 to 10 km with an average of 7.8 km. Vertical speed ranges from 0.5 to $17.8 \times 10^5$ m/s with an average of $4.0 \times 10^5$ m/s. Vertical speed is closely related with initiation altitude, with IC flashes initiated at higher altitude having lower vertical speed during PB stage. Characteristics of PB pulse trains including pulse rate, pulse amplitude, and pulse width are also analyzed. The relationship between pulse rate and vertical speed has the strongest correlation, suggesting that each PB pulse corresponds to one step of the initial leader during the PB stage. Pulse rate, pulse amplitude, and pulse width all show decreasing trends with increasing initiation altitude and increasing trends with increasing vertical speed. Using a simple model, the step length of the initial leader during the PB stage is estimated. Most of initial leaders have step lengths that range from 40 to 140 m with an average of 113 m. Estimated step length has a strong correlation with initiation altitude, indicating that leaders initiated at higher altitude have longer steps. Based on the results of this study, we speculate that above certain altitude (~12 km), initial leaders in PB stages of IC flashes may only have horizontal propagations. PB processes at very high altitude may also have very weak radiation, so detecting and locating them would be relatively difficult.

## 1. Introduction

Lightning flashes typically start with a preliminary breakdown (PB) stage which is characterized by a train of bipolar pulses in electric field change (*E*-change) records. PB is also commonly referred to as initial breakdown [e.g., *Karunarathne et al*., 2013; *Marshall et al*., 2013; *Stolzenburg et al*., 2013]. Due to the fact that PB processes occur inside the cloud, analyzing far-field *E*-change waveforms had been one of the few ways to understand the physical processes behind PB for many years [e.g., *Gomes et al*., 1998; *Nag and Rakov*, 2008; *Wu et al*., 2013]. Recently, channel developments during PB stages have been observed visually using high-speed video cameras [*Stolzenburg et al*., 2013, 2014; *Campos and Saba*, 2013], and some new insights on PB processes have been obtained. *Stolzenburg et al*. [2013] observed bursts of luminosity during the PB stages in 15 cloud-to-ground (CG) and intracloud (IC) flashes. They found that PB pulses in the *E*-change data are coincident with light bursts in high-speed video data, and they suggested that each PB pulse "is caused by a substantial current surge that is hundreds of meters long." As a follow-up study, *Stolzenburg et al*. [2014] further analyzed the PB stage of a single-stroke CG flash and found that the burst luminosity was directly related to the amplitude of PB pulses. *Campos and Saba* [2013] observed the leader processes of a negative CG flash with time-correlated high-speed video camera and electric field sensors. They showed that as the leader progressed from the initial leader in the PB stage to the stepped leader, the speed decreased from about $12 \times 10^5$ m/s to about $3 \times 10^5$ m/s and the channel luminosity also reduced.

High-speed video observations can show detailed development features of PB processes, but they are very rare due to the visibility limitation of video. Another convenient way of studying PB is using an electric field sensor network to locate PB pulses. Three-dimensional (3-D) locating of PB pulses has recently been realized by *Bitzer et al*. [2013] and *Karunarathne et al*. [2013]. *Bitzer et al*. [2013] developed a network called Huntsville

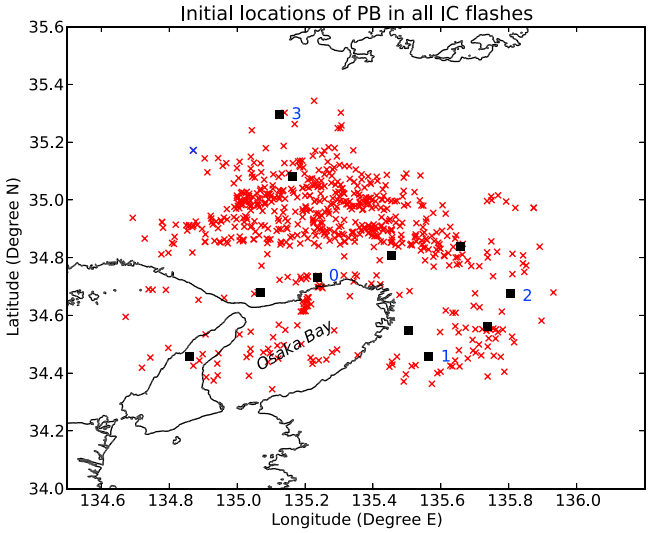


**Figure 1.** Initial locations of PB processes in IC flashes analyzed in this paper. The blue cross sign represents the initial location of an IC flash shown in more detail in Figure 2. The black squares show the locations of BOLT sites. Numbered sites will be used specifically in following analyses.

Alabama Marx Meter Array comprising seven *E*-change sensors working in the frequency band of 1 Hz to 400 kHz. They reported 3-D locations of two IC flashes which showed upward propagation with vertical speed of $7.6 \times 10^5$ m/s and $1.8 \times 10^5$ m/s, respectively, during the PB stage. They also reported a negative CG flash which propagated downward with a vertical speed of $2.2 \times 10^5$ m/s during the PB stage. *Karunarathne et al.* [2013] analyzed 3-D locations of PB pulses in several IC and CG flashes and concluded that locations of PB pulses in IC flashes show an upward propagation trend while those in CG flashes show a downward propagation trend. *Marshall et al.* [2013] analyzed PB stages in 10 IC flashes which may be associated with terrestrial gamma ray flashes. They demonstrated that PB pulses are a manifestation of the initial breakdown processes and the upward motion of negative charges from the main negative charge region to the upper positive charge region. These recent studies established that PB pulses in IC flashes are produced by the initial negative leader which propagates upward from the main negative charge region to the upper positive charge region.

IC flashes can also been initiated by narrow bipolar events (NBEs, also called compact intracloud discharges) [*Rison et al.*, 1999; *Wu et al.*, 2014]. The initial stages of these IC flashes are very similar to PB stages of normal IC flashes, both associated with positive pulse trains whose locations show upward propagation. The only difference is that the first pulse in the initial stage of a NBE-initiated IC flash is produced by a NBE while the first pulse in a PB pulse train has no apparent differences with the rest of pulses. *Wu et al.* [2014] demonstrated that characteristics of the leader processes initiated by NBEs have close connections with NBE altitude. Leaders initiated by higher NBEs tend to produce weaker pulses, propagate upward for longer durations and with slower speeds than those initiated by lower NBEs, and there are few NBE-initiated leaders above about 10 km altitude. Considering the similarities between pulse trains observed in IC flashes initiated with and without a NBE, it is expected that the properties of initial leaders associated with PB pulses in IC flashes will also vary with their initiation altitudes. However, studies on the different properties of initial leaders or PB pulses at different altitudes are still very rare. Even 3-D location results of PB pulses are still rare, and there have not been any statistical studies on altitude-related PB properties.

In this paper, we will analyze 3-D location results of 662 PB pulse trains in IC flashes. Using this large data set, first we will confirm the altitude and propagation characteristics of initial leaders during the PB stage of IC flashes. Then we will explore the possible relations between initiation altitude, propagation characteristics, and waveform characteristics of PB pulse trains. Finally, we will estimate the step length of the initial leader during the PB stage using a simple model. We will demonstrate that various properties of PB processes are closely related with their initiation altitude and upward propagation speed.

## 2. Experiment and Data

During the summer of 2013, we deployed a low-frequency (LF) lightning location network called Broadband Observation network for Lightning and Thunderstorms (BOLT) in Osaka area of Japan. This system comprised 11 sites as shown by black squares in Figure 1. Distances between adjacent sites ranged from 11 to 40 km. Each site consisted of a fast antenna with a time constant of 200 μs and effective frequency band of about 800 Hz to 500 kHz. *E*-change signals of lightning discharges were digitized at a sampling rate of 4 MS/s and

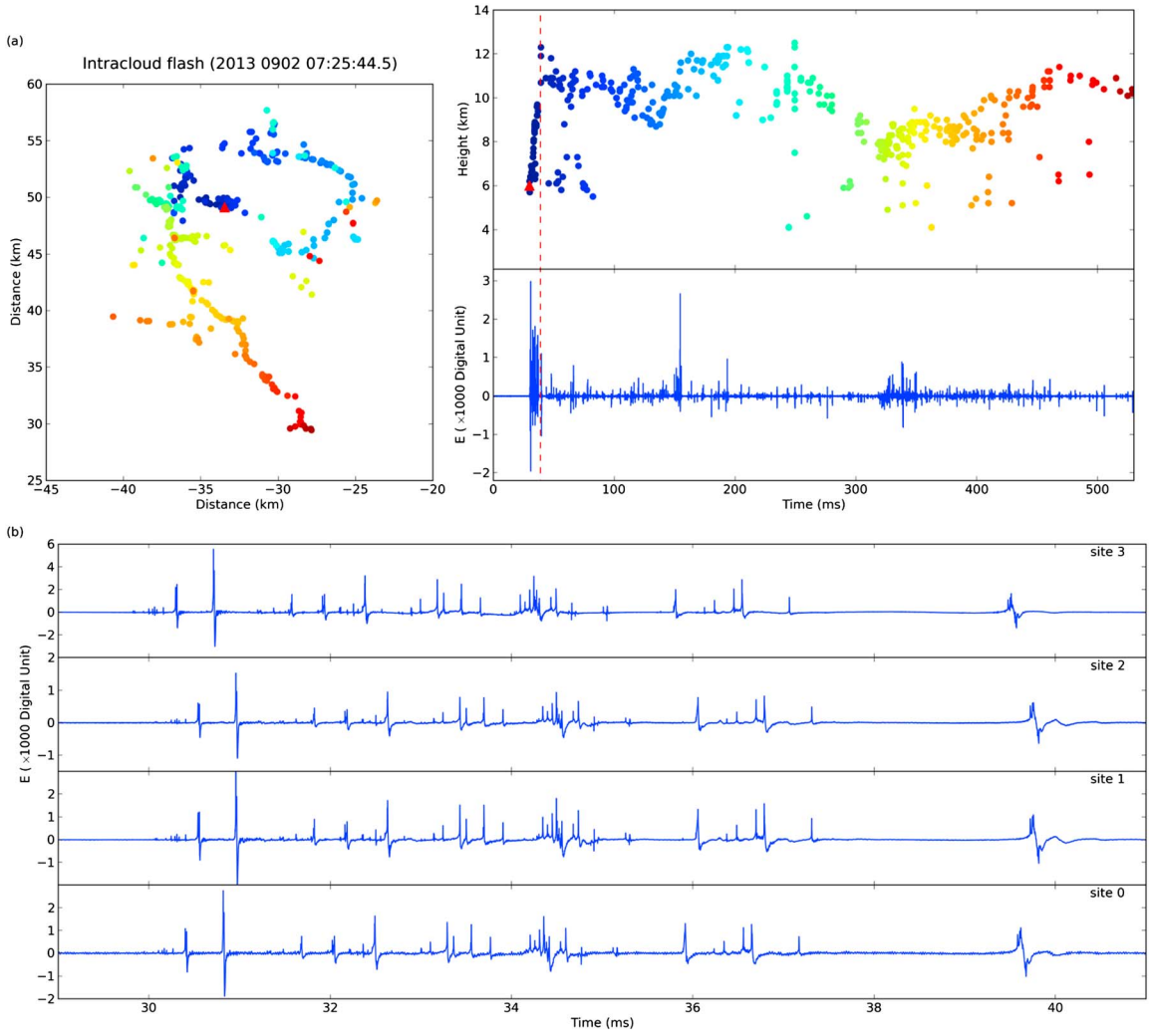


**Figure 2.** A typical example of an IC flash with PB pulses. (a) Locations and *E*-change waveform of an IC flash initiated with PB processes. The red triangle represents the location of the first pulse. The period before the red dashed line is the PB stage. The origin in the left plot (0,0) is set at the location of site 0 in Figure 1. The same origin is used in all similar figures in this paper. (b) *E*-change waveforms of the PB pulses of this IC flash recorded at four numbered sites in Figure 1.

with a vertical resolution of 16 bit. Each trigger had a duration of 200 ms and was time-stamped by a GPS receiver with a timing accuracy of 50 ns. This system can be continuously triggered without any deadtime. Time-of-arrival technique was employed to obtain 3-D locations of lightning discharges as described in *Yoshida et al*. [2014].

In this study, we will analyze 3-D locations and *E*-change waveforms of PB pulses. Figure 2a shows 3-D locations and *E*-change waveform of a typical IC flash, the initial location of which is shown as a blue cross in Figure 1. The portion of the flash occurring before the red dashed line is PB stage. During the PB stage of this flash, an initial leader propagated upward, presumably carrying negative charge from the main negative charge region to the upper positive charge region. After the PB stage, the location results mainly showed the development of the negative leader in the upper positive charge region. There were also a few sources in the main negative charge region, probably produced by negative recoil and/or positive leaders. The leaders progressed mainly horizontally, forming several clear branches spanning more than 20 km.

Figure 2b shows *E*-change waveforms of the PB stage recorded at the four numbered sites in Figure 1 (waveforms recorded by other sites are not shown). All of the pulses are of positive polarity as in physics sign convention. In practice, for the beginning part of a PB pulse train, if the pulses at one site are positive, they are also positive at all the other sites, indicating that the initial leader starts with mainly vertical development. The PB stage usually

ends with pulses at several sites starting to change polarity, which is probably caused by horizontal propagation of the initial leader. The PB stage of this flash lasted for about 10 ms. Based on these characteristics, we set the following criteria to identify PB processes.

1. *A PB pulse train should appear at the beginning of an IC flash*. This does not necessarily mean that there are no *E*-change signals before PB pulses as these signals can be produced by discharge processes far away from the PB processes, but we can exclude these signals by their locations. If two leaders develop consecutively from nearby locations such as the case discussed by *Winn et al*. [2011] and the one shown in Figure 5b in *Wu et al*. [2014], only the first leader is considered.
2. *There should be at least five positive pulses from the start of the pulse train before any negative pulse appears at any site*. Five is a somewhat arbitrary setting, but in most of the cases, the initial leader produces many more than five pulses. If a site is very close to a flash ($<$10 km) and waveforms at this site are highly distorted due to the large static component, pulse polarities at this site are not considered.
3. *Locations of the PB pulses should show an upward propagation trend*. Not all PB processes in IC flashes show upward propagation, but calculating upward propagation speed is an essential part in this study. This criterion makes the flashes in this study basically normal positive IC flashes.

In order to ensure high location accuracy, only those flashes that were located near the center of the BOLT array, and occurred when all 11 sites were operating normally, were included for analysis. In total, 662 flashes with PB processes are identified, and their initial locations are shown in Figure 1. These PB processes occurred inside or quite near the array, and the vertical error of their location results is typically less than 500 m (Figure 5 in *Yoshida et al*. [2014]). A large number of these flashes are located in the northern region of the array, where a mountainous area is conducive to the formation of thunderstorms in the summer.

In addition, PB pulses in negative CG flashes are identified for a comparison in section 3.1. Negative CG flashes that occurred in the same period and region as described above are considered. If there are at least five negative pulses at the beginning of a negative CG flash before any positive pulse appears at any site, these negative pulses are identified as a PB pulse train in negative CG flash. In total, 558 negative CG flashes with PB pulses are identified.

## 3. Results

### 3.1. Initiation Altitude of PB

One of the most important properties of PB is its initiation altitude, which is related to the origin of lightning flashes in thunderclouds. *Marshall et al*. [2014] reported that they detected a type of slow and small *E*-change signals called initial *E* changes (IECs) before the beginning of PB pulses. In most PB cases in this study, we cannot find IECs before them probably because IECs can only be detected within small distances (around 4 km as in *Marshall et al*. [2014]), so we will not consider IECs in this study. Considering that the IEC is a type of slow process with very small dipole moment and short duration, there should not be significant charge motions during the IEC, so we state that the initial location of PB is a good proxy of lightning initiation location.

We calculated the altitude of the first pulses in PB pulse trains as their initiation altitude, and as a comparison, we also calculated initiation altitude of PB pulses in 558 negative CG flashes. Figure 3 shows time series (Figure 3, left) and a distribution (Figure 3, right) of the initiation altitude of PB in all IC and CG flashes. The green dashed lines divide different thunderstorm days. Altitudes of 0°C, −10°C, −20°C, and −40°C isotherms in each day are also plotted. The isotherm altitudes are obtained by radiosonde observations by Japan Meteorological Agency at Shionomisaki, which is about 150 km from the center of our network, and are only available for 09:00 A.M. and 09:00 P.M. local time each day. Therefore, these data provide only an extremely rough estimation of the temperature inside the thunderclouds.

We can see some interesting patterns in Figure 3. First, initiation altitude of PB in ICs is generally higher than that in negative CGs. Second, as in days 0727, 0731, 0805, and 0807, PB of most ICs is higher, and most CGs lower, than the −10°C isotherm. It seems that the main negative charge regions of these thunderstorms reside near the −10°C level, which is a reasonable temperature level for the main negative charge region [e.g., *Krehbiel*, 1986]. Other thunderstorms seem to be more complicated. Particularly, we can see that PB in some IC flashes is initiated below the 0°C isotherm. It is possible that these IC flashes are initiated at temperatures higher than 0°C, which may be difficult to explain using the graupel-ice mechanism [e.g., *Takahashi*, 1978]

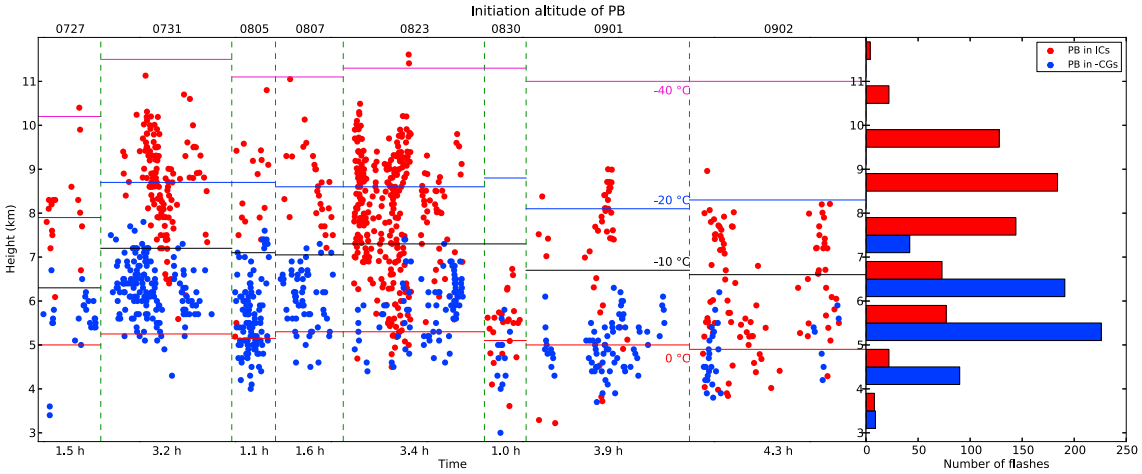


**Figure 3.** Initiation altitude of PB in IC flashes and negative CG flashes. (left) The time series of PB altitude in all thunderstorm days analyzed in this study. Different thunderstorm days are divided by the green dashed lines. The numbers above the figure show the dates and those below the figure the durations of all PB processes in each day. The red, black, blue, and purple lines indicate the 0°C, −10°C, −20°C, and −40°C isotherms, respectively. (right) The distribution of initiation altitude of PB in all flashes.

as it requires supercooled water for substantial charge separations. However, this may just reflect the fact that the actual charge structure in a thundercloud can be much more complicated than a simple tripolar structure [*Stolzenburg et al*., 1998]. It is also possible that the region with strongest electric field, where lightning is initiated, is sometimes displaced from the active charging region where supercooled water is necessary. Lightning flash origins are probably also dependent on types and stages of thunderstorms, and fully understanding lightning initiation locations requires detailed analysis of thunderstorm structures, which is outside of the scope of this paper.

Figure 3 (right) shows the distribution of initiation altitude of PB for all flashes. The PB for most negative CG flashes is initiated between 4 and 7 km with an average value of 5.7 km. The PB for most IC flashes is initiated between 5 and 10 km with an average value of 7.8 km. The overall results in Figure 3 are consistent with the notion that IC flashes are initiated between the main negative and upper positive charge regions and that the initial leaders propagate upward. Conversely, negative CG flashes are initiated below the main negative charge region, and their initial leaders propagate downward toward the ground.

### 3.2. Upward Propagation Speed

PB pulses are produced by initial leaders, which propagate upward in normal positive IC flashes [e.g., *Marshall et al*., 2013]. Speeds of initial leaders were previously observed by VHF lightning imaging systems. For example, using a 2-D interferometer system, *Shao and Krehbiel* [1996] observed that initial leaders in IC flashes propagated upward at a speed of 1.5 to $3 \times 10^5$ m/s. *Behnke et al*. [2005] reported that initial leaders in IC flashes started at a median speed of about $1.6 \times 10^5$ m/s using data obtained by lightning mapping array (LMA). *Bitzer et al*. [2013] compared speed values calculated from VLF/LF and VHF sources for two IC flashes and two CG flashes and found that these two types of sources gave very similar results. In this section, we will present an analysis of upward propagation speed for initial leaders during the PB stage in all 662 IC flashes. First, we will consider the vertical speed component.

Figures 4a–4d show four basic types of upward propagation during the PB stage, and they illustrate the method used to calculate the vertical speed. In each case, the slope of the red dashed line is the estimated vertical speed. The red dashed line represents a least squares linear fit to a subset of the height and time of PB pulses with a fixed point at the height and time of the first PB pulse. The subset includes all PB pulses between the first located PB pulse and a manually selected final pulse. The selection of the final pulse is illustrated in Figures 4a–4d. PB of type 1 (Figure 4a) propagates vertically at a relatively constant speed and then turns horizontal; final source is when the channel turns horizontal. PB of type 2 (Figure 4b) propagates vertically with a speed that decreases with height (similar to the cases reported by *Behnke et al*. [2005]); final source is when the initial leader reaches about two thirds of its maximum height. The maximum

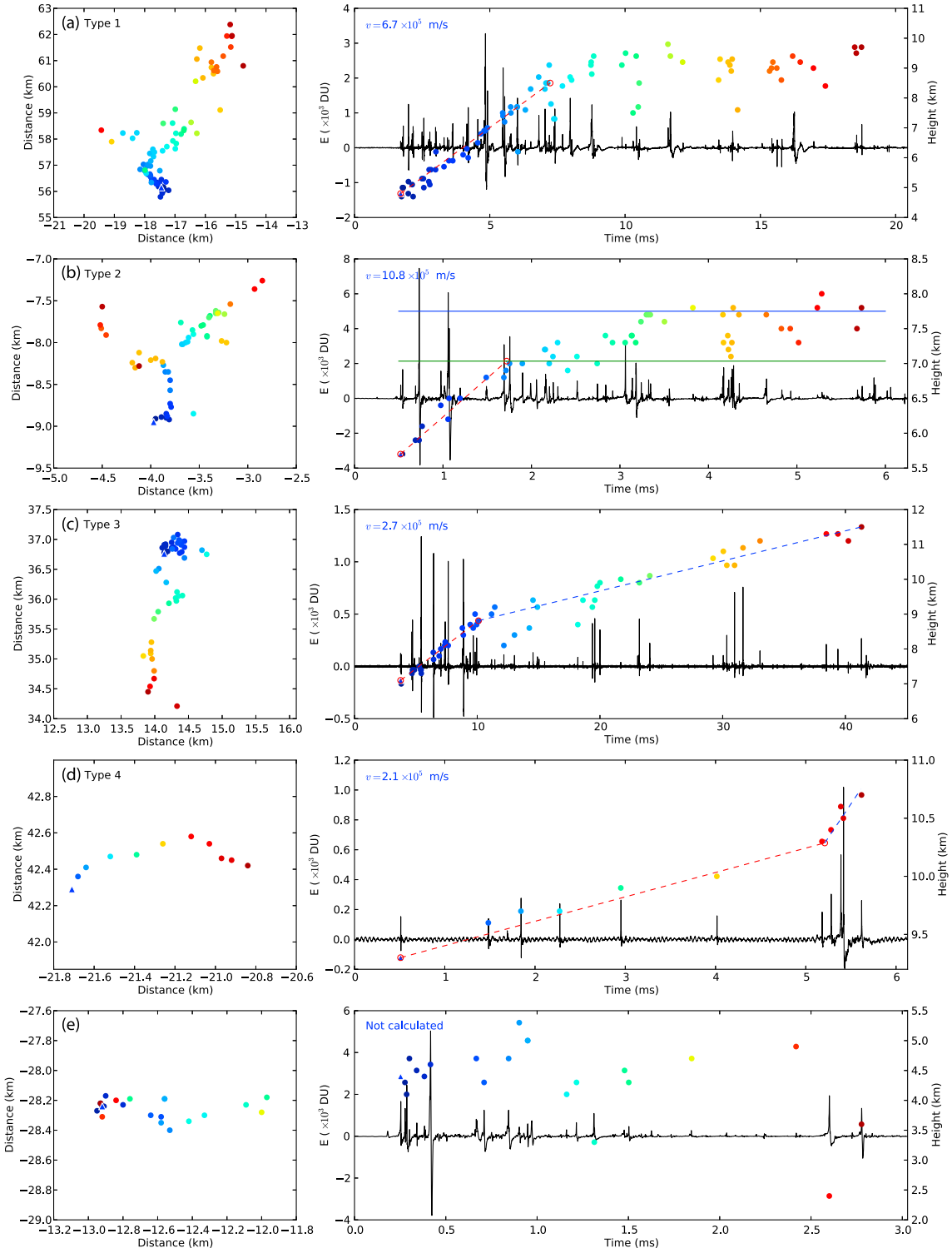


**Figure 4.** (a–e) Illustration of the calculation of vertical speed. In each figure, the left part shows *x-y* results and the right part shows height-time results along with the *E*-change waveform at one site. Slopes of dashed red lines are estimated vertical speed. In Figure 4b the blue line indicates the top height of the development of the initial leader and the green line indicates the two-third top height level. The blue dashed lines in Figures 4c and 4d indicate the second stages.

and two-third maximum height are indicated by the blue and green lines, respectively. PB of type 3 (Figure 4c) propagates upward in two stages, with the first stage faster than the second; final source is at the end of the first stage. PB of type 4 (Figure 4d) also propagates vertically in two stages, but the first stage is slower than the

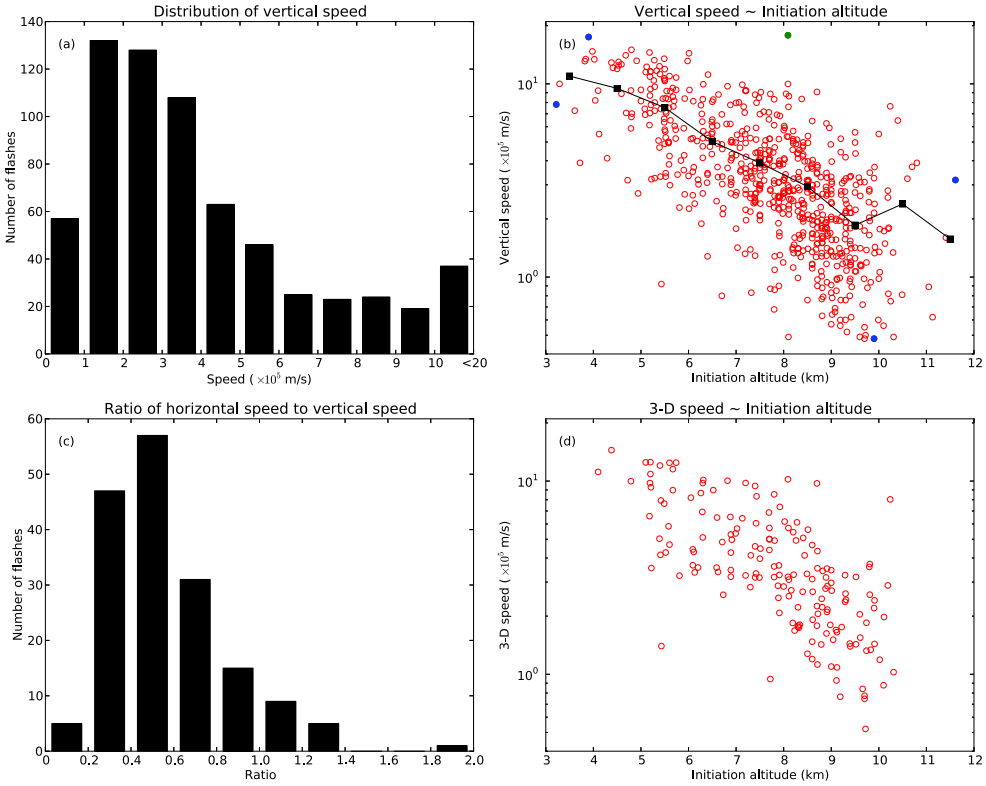


**Figure 5.** (a) Distribution of vertical speed. (b) Scatterplot of vertical speed versus initiation altitude of PB. The black squares represent the average speed in each kilometer bin of altitude. The PB cases represented by blue dots are shown in Figure 6, and the one represented by a green dot is shown in Figure 8c. (c) Distribution of the ratio of horizontal speed to vertical speed. (d) Scatterplot of 3-D speed versus initiation altitude of PB.

second; final source is at the end of the first stage. There are also cases in which no clear upward propagation trend can be determined, as shown in Figure 4e. It is not clear if the lack of apparent vertical motion is due to the initial leader propagating only horizontally or due to limitations in vertical location accuracy, so these cases are excluded from this study.

It should be noted that the classification of four types of PB in Figure 4 is not strict; sometimes it is difficult to determine which type a PB process belongs to. The manual determination of the final pulse for speed calculation may also introduce certain errors, but these errors should not be significant. Cases we had difficulty making the linear fit are not used such as the one in Figure 4e. The above method illustrates our purpose to calculate the speed over the beginning period of the PB stage, during which the vertical speed does not have large variations so that we can make the linear fit. The vertical speed can change significantly as the initial leader develops during the PB stage, and the relatively constant vertical speed at the beginning part of the initial leader is used. We believe that this is the best way of calculating the vertical speed for comparison of PB stages in hundreds of IC flashes. Further, speed calculated in this way is most likely associated with the initiation altitude; the association will be analyzed later in this section.

With the above method, we calculated the vertical speed for the PB of all 662 IC flashes. The results are summarized in Figure 5. Figure 5a shows the distribution of vertical speed. The distribution shows highest percentages between 1 and $4 \times 10^5$ m/s, which is consistent with previous studies [*Shao and Krehbiel*, 1996; *Behnke et al*., 2005; *Bitzer et al*., 2013]. The average speed is $4.0 \times 10^5$ m/s, and the maximum and minimum values are $17.8 \times 10^5$ m/s and $0.5 \times 10^5$ m/s, respectively. Note that there are many flashes having quite large speed during the PB stage, some of which are larger than $10 \times 10^5$ m/s. High speed is related to low initiation altitude as illustrated in Figure 5b, which shows a scatterplot of vertical speed versus initiation altitude. The speed has a clear decreasing trend as the initiation altitude increases. Here we use the Spearman's rank correlation coefficient to quantitatively describe the correlation between two variables. The Spearman's correlation

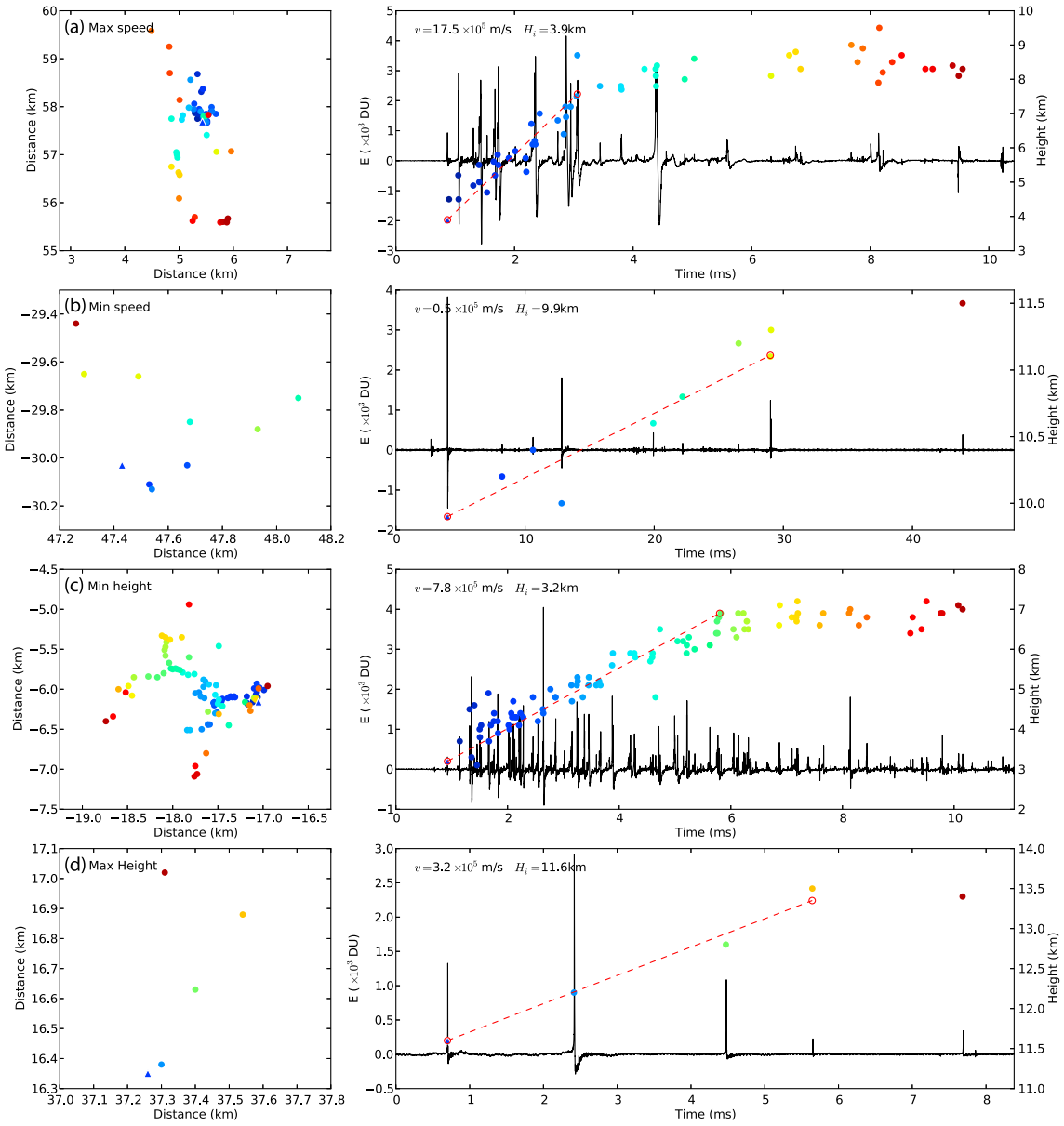


**Figure 6.** Locations and *E*-change waveforms of PB with the (a) fastest upward propagation, (b) slowest upward propagation, (c) lowest initiation altitude, and (d) highest initiation altitude. Slopes of dashed red lines are estimated vertical speed.

coefficient is more appropriate to describe nonlinear relations than the normal Pearson's correlation coefficient. The Spearman's correlation coefficient is −0.68 for initiation altitude and speed in Figure 5b. The black squares in Figure 5b represent average speeds in each kilometer bin of altitude. The average speed decreases from $11.0 \times 10^5$ m/s for PB lower than 4 km to $1.6 \times 10^5$ m/s for PB higher than 11 km. The only increase of the average speed is in 10~11 km range, which may be due to the small number of samples in this range. This result indicates that initial leaders started at higher altitude tend to propagate upward with lower speed.

Next we will briefly examine the horizontal speed component. The horizontal propagation of initial leaders is highly varied; sometimes we cannot recognize a clear propagation direction, and sometimes there seems to be branches. We examined locations of all PB processes in this study and calculated horizontal speed component for PB in 170 flashes, all of which show clear and simple horizontal propagations. Horizontal speed is calculated in the same period of each flash as the calculation of vertical speed illustrated in Figure 4. Figure 5c shows the distribution of the ratio of horizontal speed to vertical speed. The distribution peaks

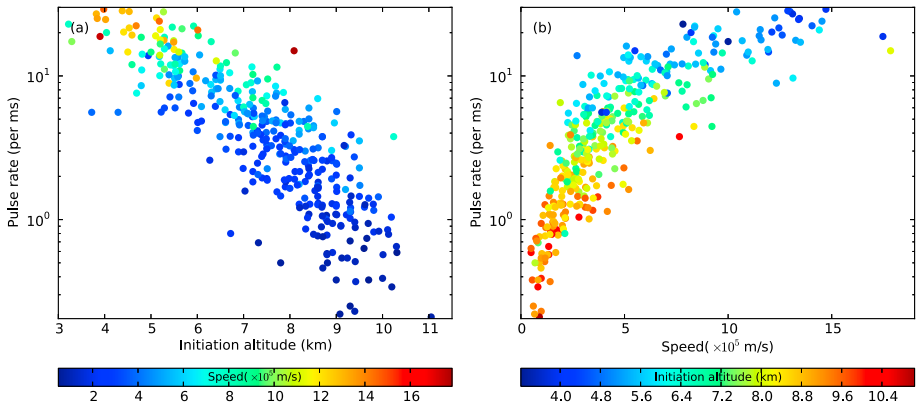


**Figure 7.** Relations between pulse rate, initiation altitude, and vertical speed of PB. (a) Scatterplot of pulse rate versus initiation altitude with color indicating speed. (b) Scatterplot of pulse rate versus speed with color indicating initiation altitude.

around 0.5, indicating that for PB stages in IC flashes, horizontal speed of the initial leader is usually only about half of its vertical speed. For PB in most IC flashes (91.2%), horizontal speed of the initial leader is smaller than its vertical speed. We also calculated 3-D speed for these cases by combining horizontal and vertical speed components. Figure 5d shows a scatterplot of 3-D speed versus initiation altitude. It shows a very similar trend to the relationship between vertical speed and initiation altitude (Figure 5b). The mean value of 3-D speed is $4.3 \times 10^5$ m/s. In the following analysis, we will only consider the vertical speed component because the vertical speed is probably more closely related with initiation altitude and charge structures in thunderstorms. Note that when we talk about "upward propagation speed" in following text, we only refer to the vertical speed component.

Both initiation altitude and speed of PB vary over a wide range. It is instructive to examine the extreme cases in more detail. Figure 6 shows 3-D locations and *E*-change waveforms of PB with the largest and smallest vertical speeds and initiation altitudes (blue dots in Figure 5b). Note that in Figure 5b, the largest speed is $17.8 \times 10^5$ m/s occurring at 8.1 km altitude (green dot in Figure 5b). However, this case is a quite special case and will be discussed later in section 3.3.1. Except for this case, the largest speed is $17.5 \times 10^5$ m/s, which is shown in Figure 6a. It is initiated at an altitude of 3.9 km. Figure 6b shows the PB with the smallest speed ($0.5 \times 10^5$ m/s), and it is initiated at an altitude of 9.9 km. Note that there is a small pulse before PB pulses, which is produced by a distant lightning discharge. Figures 6c and 6d show PB with the smallest (3.2 km) and largest (11.6 km) initiation altitudes, respectively. These two cases show clear upward propagation with speeds of $7.8 \times 10^5$ m/s and $3.2 \times 10^5$ m/s, respectively. These examples reflect the result in Figure 5b that initial leaders with high initiation altitude usually propagate upward more slowly while those with low initiation altitude usually propagate upward more quickly.

### 3.3. Pulse Train Characteristics

PB in normal positive IC flashes produces positive bipolar pulses. There have been many studies analyzing characteristics of PB pulse trains [*Ushio et al.*, 1998; *Gomes et al.*, 1998; *Gomes and Cooray*, 2004; *Makela et al.*, 2008; *Baharudin et al.*, 2012]. Here we present a statistical analysis on characteristics of PB pulse trains in IC flashes, paying special attention to their association with initiation altitude and upward propagation speed.

#### 3.3.1. Pulse Rate

From PB examples in Figure 6, we can notice an interesting feature. It seems that PB initiated at higher altitude and with slower speed (Figures 6b and 6d) produces fewer pulses than PB initiated at lower altitude and higher speed (Figures 6a and 6c). In order to examine this feature, we will calculate pulse rate of PB pulse trains and investigate its relations with PB initiation altitude and upward propagation speed. Pulse rate is defined as the number of PB pulses per unit time. If multiple pulses are detected within a 5 μs window, only the largest pulse is counted as these pulses are probably multiple peaks of the same PB pulse. Every PB pulse train is recorded by multiple sites, and in order to avoid systematic differences between waveforms recorded at different sites, for this analysis we will only use *E*-change waveforms recorded by site 1 in Figure 1. In addition, pulses produced by very close discharges may be seriously distorted due to static field component, so here we

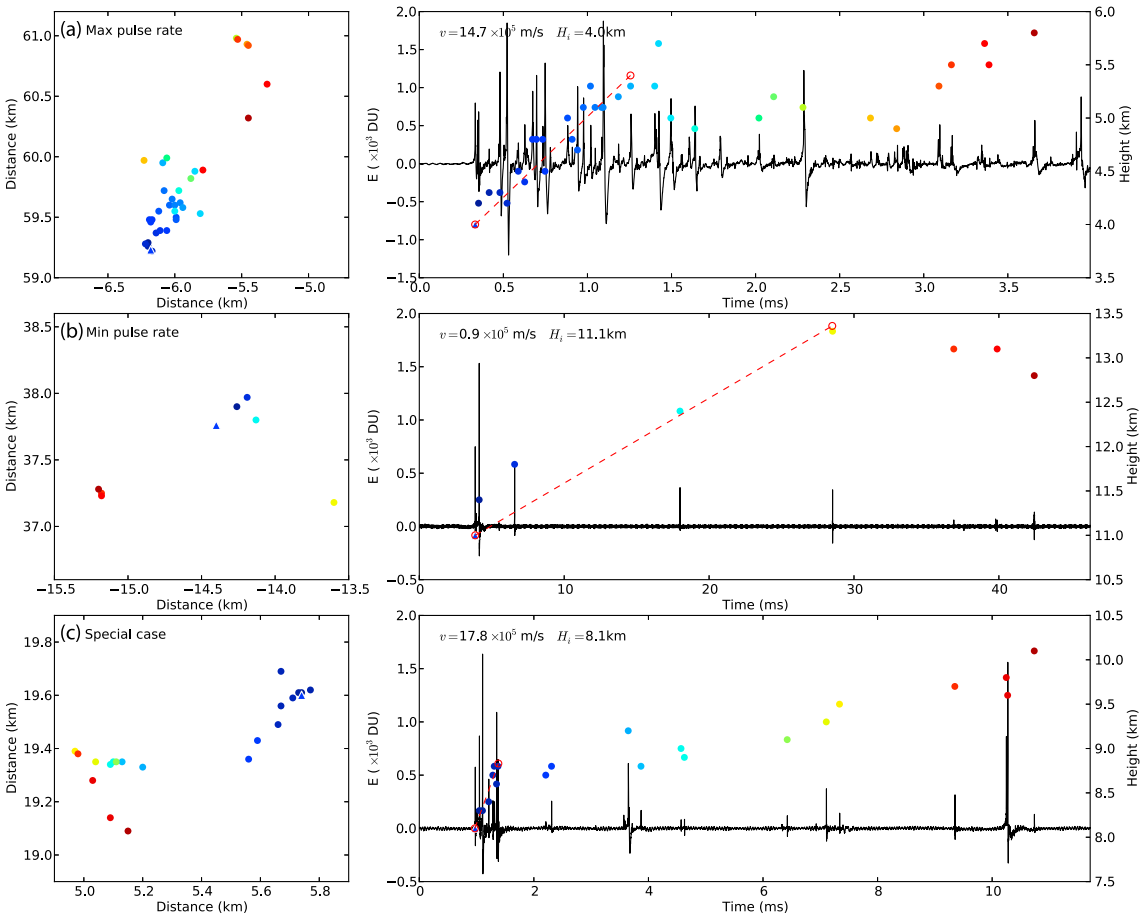


**Figure 8.** Locations and *E*-change waveforms of PB pulse trains with (a) largest pulse rate, (b) smallest pulse rate, and (c) a special case which has the highest speed. Slopes of dashed red lines are estimated vertical speed.

only include PB processes at least 50 km away from site 1. These standards limit this analysis to the PB in 365 flashes. The pulse rate is calculated over the same period used for the upward speed calculation (red dashed lines in Figure 4).

Figure 7 shows the relations between pulse rate of PB pulse trains and their initiation altitude and upward propagation speed. Figure 7a is a scatterplot of pulse rate versus initiation altitude with color indicating the speed, and Figure 7b is a scatterplot of pulse rate versus speed with color indicating the initiation altitude. In Figure 7a we can see as the initiation altitude increases, the pulse rate decreases, and for PB cases with the same initiation altitude, those having higher pulse rate generally have higher speed. Figure 7b shows similar results. As speed increases, pulse rate also increases, and for PB cases with the same speed, those having higher pulse rate generally have lower initial height. The Spearman's correlation coefficient is −0.86 for pulse rate and initiation altitude and 0.88 for pulse rate and speed. In conclusion, PB initiated at lower altitude or propagating with higher vertical speed generally produces pulses more frequently.

To further illustrate the above results, some PB examples are shown in Figure 8. The PB in Figure 8a has the highest pulse rate, quite a large upward propagation speed, and a relatively low initiation altitude. On the other hand, the PB in Figure 8b has the lowest pulse rate, a relatively low propagation speed, and a high initiation altitude. The PB in Figure 8c is a special case. It has the highest propagation speed but also a relatively high initiation altitude, which seems to contradict our conclusion in section 3.2 (PB with high initiation altitude tends to have low propagation speed). The reason is that this PB starts with many pulses within a short period, and in this period, it propagates upward very rapidly. After this period, the pulses are much less frequent and the speed also decreases. This is type 3 PB as shown in Figure 4c, and its speed is calculated for the first upward propagation stage as indicated by the red dashed line. This example further illustrates

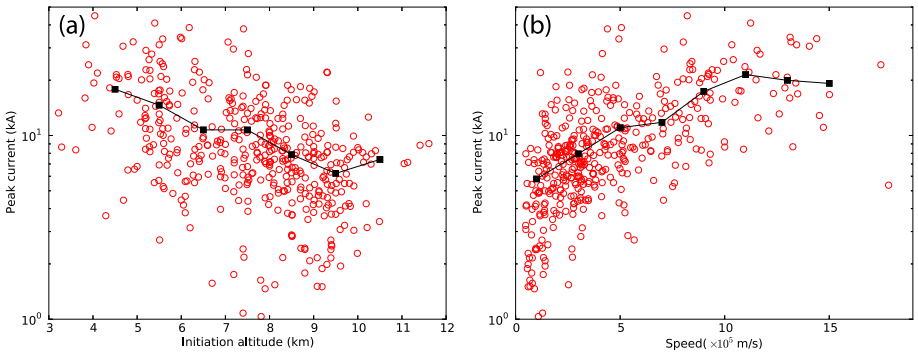


**Figure 9.** Relations between estimated peak current, initiation altitude, and upward propagation speed of PB pulse trains. (a) Scatterplot of peak current versus initiation altitude. (b) Scatterplot of peak current versus speed. The black squares represent the average values.

the result that more frequent pulses correspond to higher upward propagation speed. A similar feature can also be seen in the type 4 PB in Figure 4d. Here the first stage has a relatively small speed and sparse pulses, and the second stage has a larger speed and more frequent pulses. It seems that pulse rate is more closely associated with upward propagation speed than with initiation altitude.

### 3.3.2. Pulse Amplitude

In this section, we will investigate characteristics of PB pulse amplitude for PB pulse trains with different initiation altitudes and upward propagation speeds. In order to compare the amplitude of PB pulses at different distances, we convert the *E*-change records to estimated peak current using the method presented in *Wu et al*. [2014]. This method is based on the transmission line model mainly applicable to return strokes, so the estimated current values of PB pulses may not be accurate. However, the method will be correct for the amplitude falloff with distance of the radiation component of the electric field. For this analysis, only PB processes located more than 50 km from site 2 or site 3 are considered, the same as the treatment in *Wu et al*. [2014]. This limits the sample size to the PB pulse trains in 443 flashes. For each PB pulse train, the peak current is found from the PB pulse with the largest amplitude.

Figure 9 shows relations between estimated peak current of PB pulse trains, initiation altitude, and upward propagation speed. The black squares represent average values of peak current in (a) 1 km bin of altitude and (b) $2\times10^5$ m/s bin of speed. We can see that as the initiation altitude increases, the peak current shows a decreasing trend, although the scatter is very large. The Spearman's correlation coefficient is −0.46. The relation between peak current and speed is stronger, with the Spearman's correlation coefficient of 0.64. PB initiated at lower altitude and with larger upward propagation speed tends to produce larger PB pulses.

### 3.3.3. Pulse Width

Many studies on PB pulse trains analyzed PB pulse widths [e.g., *Ushio et al*., 1998; *Gomes and Cooray*, 2004]. We will also make a statistical analysis on pulse width of PB in IC flashes and investigate if it has any association with initiation altitude or upward propagation speed. Data used in this analysis are the same as that used for the analysis of pulse rate in section 3.3.1. For each of 365 pulse trains, the width of all pulses is calculated (from 10% peak at the leading edge to zero crossing) and then averaged. The distribution of the average pulse width is shown in Figure 10a, showing highest percentages between 5 and 20 μs with an average value of 15.3 μs. This is generally longer than pulse widths in positive and negative CG flashes reported in previous studies [*Gomes and Cooray*, 2004; *Baharudin et al*., 2012; *Wu et al*., 2013]. It is also consistent with the report by *Bitzer et al*. [2013] that PB pulses in IC and hybrid flashes have longer pulse durations than those in negative CG flashes.

Figures 10b and 10c explore associations of pulse width with initiation altitude and upward propagation speed of PB. The black squares represent average value of pulse width in (a) 1 km bin in altitude and (b) $2\times10^5$ m/s bin in speed. The relation between pulse width and initiation altitude is not strong with the Spearman's correlation coefficient of −0.32, although the average values show a general decreasing trend. The relation between pulse width and speed is stronger with the Spearman's correlation coefficient of 0.49. It is evident that PB with high speed usually produces pulses with long widths and PB producing pulses with short widths mostly has slow speed.

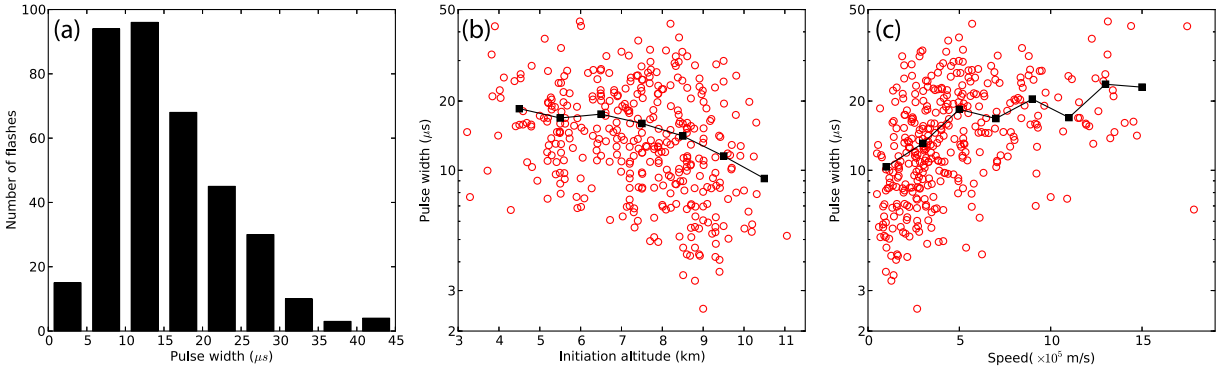


**Figure 10.** Pulse width of PB pulse trains in IC flashes. (a) Distribution of average pulse width. (b) Scatterplot of pulse width versus initiation altitude. (c) Scatterplot of pulse width versus upward propagation speed. *Y* axes in Figures 10b and 10c are logarithmic scales.

### 3.4. Step Length Estimation

Section 3.3.1 demonstrated a very strong association between the pulse rate of PB pulse trains and upward propagation speed, which is consistent with the hypothesis that each PB pulse is produced by a stepping of the initial leader. *Stolzenburg et al.* [2014] made a detailed discussion on whether the initial leader is a stepped leader. They presented evidence both supporting and contradicting the idea. They also proposed a hypothesis that initial leaders may step in an unusual way; their steps "are driven primarily by large ambient electric field and occur in the absence of a hot channel." *Stolzenburg et al.* [2013] observed that each PB pulse was coincident with light burst from the initial leader, and they suggested that there are repeated initial leaders during the PB stage with each initial leader ending with an impulsive breakdown event, which produces a PB pulse.

If we assume that the initial leader producing PB pulses is indeed stepped (even though its physical mechanism may be different from normal stepped leaders), we can estimate the average step length ($l$) of an initial leader from PB pulse rate ($\rho$; analyzed in section 3.3.1) and upward propagation speed ($v$; analyzed in section 3.2) with the following relationship:

$$l = v/\rho \tag{1}$$

Note that equation (1) also assumes that the initial leader does not have any branch and the estimated step length $l$ is only in the vertical direction. Also note that $v$ and $\rho$ should be calculated using the same period in each PB pulse train; otherwise, equation (1) may not be true.

With the relationship in equation (1), we calculated step length using data of PB pulse rate and upward propagation speed shown in Figure 7. Figure 11a shows a distribution of the estimated step length. Note that the bins are not equally distributed. Estimated step length varies over a large range, from 20 to 426 m, with an average value of 113 m. We can see from Figure 11a that the highest percentages are around 40 to 100 m and the majority (81.9%) is smaller than 160 m.

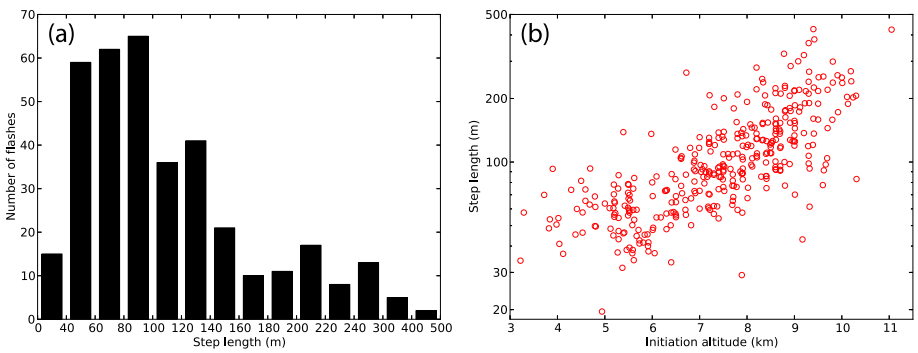


**Figure 11.** (a) Distribution of estimated step length. Note that the bins are not equally distributed. (b) Scatterplot of estimated step length versus initiation altitude. The *Y* axis is a logarithmic scale.

**Table 1.** Spearman's Correlation Coefficient Between Different Pairs of Variables

| | Vertical Speed | Pulse Rate | Peak Amplitude | Pulse Width | Step Length |
|---|---|---|---|---|---|
| Initiation altitude | −0.68 | −0.86 | −0.46 | −0.32 | 0.77 |
| Vertical speed | - | 0.88 | 0.64 | 0.49 | −0.48 |

One major source of error in our calculation is the determination of pulse rate ($\rho$). It is possible that some relatively small pulses are buried in the background noise and are not detected. In this situation, our results would be overestimations. However, all flashes analyzed in this study are inside or very near the network (Figure 1), and we should be able to detect most of PB pulses in these flashes.

To the best of our knowledge, step length of initial leaders in IC flashes has not been reported in the literature. *Edens et al*. [2014] observed cloud-to-air leaders in two IC flashes with a digital still camera and the LMA. They reported that the step lengths were at least 200 m and 264 m, respectively, in two leaders. They also noted that steps of negative leaders at 10 km altitude are an order of magnitude longer than those near sea level. *Stolzenburg et al*. [2014] analyzed high-speed video observations of a negative CG flash and reported that step lengths of the initial leader ranged from 30 to 183 m with an average of 89 m. *Petersen and Beasley* [2014] made a similar observation of a negative CG flash and suggested that the initial leader in the PB stage extends with step lengths often exceeding 200 m. The above studies are all 2-D estimations of step lengths so these results should be underestimations. Our results in Figure 11a are consistent with these observations. However, in our results there are only 45 initial leaders (12.3%) with average step lengths longer than 200 m. This may be because that we are calculating average step length for each initial leader, so extremely long or short steps may not show up. Besides, leader processes analyzed in the above studies are not initial leaders in IC flashes, so it may have some problems when comparing our results directly to the above results.

Figure 11b shows a scatterplot of estimated step length versus initiation altitude of initial leaders. Step length is calculated from pulse rate and upward propagation speed (equation (1)), both of which decrease with increasing initiation altitude (Figures 5b and 7a). Conversely, step length shows a clear increasing trend with increasing initiation altitude with the Spearman's correlation coefficient of 0.77. We can see that as the initiation altitude increases, an initial leader develops upward with longer (on average) but less frequent steps (lower pulse rate) and the resultant upward propagation speed decreases.

## 4. Discussion

We have demonstrated that PB properties have close connections with initiation altitude and upward propagation speed. Table 1 summarizes Spearman's correlation coefficients between different pairs of variables of PB properties. The coefficients indicate how strong two variables are associated with each other.

*Edens et al*. [2014] gave an explanation for the correlation between step length and initiation altitude. Lower pressure and air density at higher altitude result in a longer mean free path of free electrons and larger streamer zones at the leader tip and are conducive for the production of longer steps. Therefore, step lengths of leaders at higher altitude tend to be longer. Based on the assumption that propagation speeds of negative leaders of IC and negative CG flashes are similar, *Edens et al*. [2014] explained why the rate of radio emissions from IC flashes are lower than that in CG flashes, as at lower altitude, more frequent steps (with shorter step lengths) are required to achieve a similar speed. Our results further demonstrate that for PB stages in IC flashes, radio emissions also have a lower rate at higher altitudes (correlation between pulse rate and initiation altitude). However, the propagation speed is not the same at different altitudes. Upward propagation speed decreases with initiation altitude with a correlation coefficient of −0.68. The speed of an initial leader initiated at 5 km altitude can be 1 order of magnitude higher than those initiated at 10 km altitude. It is also quite possible that initial leader speeds in IC and CG flashes are different. If this is true, the difference in the rate of radio emissions from IC and CG flashes cannot be simply attributed to the difference in step length in different altitudes as in *Edens et al*. [2014]. Instead, we think that the ambient electric field is a more important factor, which will be discussed below along with other parameters in Table 1.

Pulse rate, peak amplitude, and pulse width all have higher correlations with vertical speed than with initiation altitude. One essential factor behind these correlations may be the ambient electric field. A stronger

electric field can make electrons at the leader tip move forward more rapidly, so the speed of leader extension is larger. If each extension (or step as assumed in section 3.4) produces one PB pulse, then the PB pulse rate is also larger. Fast moving electrons also correspond to larger currents and thus larger peak amplitude of PB pulses. (As a similar process, growth of corona current was discussed by *Bazelyan and Raizer* [1998, p. 6].) A stronger electric field may also generate more electrons at the leader tip, and the current produced by leader extension may have longer duration, so the PB pulse produced by the current also has larger width. These associations may explain correlations of vertical speed with pulse rate, peak amplitude, and pulse width. The correlation between pulse rate and vertical speed has the largest coefficient (0.88). This is consistent with the observation by *Stolzenburg et al*. [2013] that each PB pulse is coincident with light burst from the initial leader, suggesting that each PB pulse corresponds to one step of the initial leader, although the initial leader steps may be physically different from normal leader steps.

Pulse rate, peak amplitude, and pulse width are all negatively correlated with initiation altitude. At higher altitude, the electric field required for initiation and leader propagation is smaller, and with the relations analyzed above, weaker electric field is associated with lower pulse rate, smaller peak amplitude, and smaller pulse width. However, the electric field does not necessarily decrease with the altitude. As the initial leader propagates upward, it may encounter regions with electric field stronger than where it is initiated. This may be one reason why these coefficients are relatively small. The correlation for pulse width is especially weak. A possible reason is that the current duration is more closely related with the amount of charge that is available for the extension of the initial leader than with ambient electric field strength. A strong electric field can also produce discharges associated with very narrow pulses such as NBEs.

*Wu et al*. [2014] reported the so-called "initiator-type NBEs (INBEs)," which occur at the very beginning of IC flashes. INBEs are followed by upward propagating leaders which produce positive pulse trains very similar to PB pulse trains. INBEs with subsequent upward propagating leaders are also similar to initial leaders in PB stages. Characteristics of positive pulse trains and corresponding leader processes following INBEs also change with initiation altitude. As shown by Figures 8 and 11 in *Wu et al*. [2014], pulse amplitude, pulse rate, and upward propagation speed all decrease with increasing initiation altitude, the same as PB processes in IC flashes. Therefore, we conclude that leader processes following INBEs are the same as initial leaders in PB stages of IC flashes. The only difference is that the INBE produces a distinguishing large bipolar pulse as the start of a flash while the first pulse of a PB pulse train is usually very small and does not have any apparent difference with other pulses. It is not clear whether the presence of an INBE has any influence on the development of the flash.

As reported by *Wu et al*. [2014], INBEs are mostly lower than 10 km. At higher altitude, there are only normal NBEs which are relatively isolated and are not followed by positive pulse trains. This feature makes us wonder whether PB processes also only exist below certain altitude. The highest initiation altitude for PB processes in this study is 11.6 km (the example in Figure 6d). It is very difficult to find flashes showing clear initiations at higher altitude. One reason may be the height limitation for thunderstorm development and charge layers, limiting the possible initiation height of lightning. Another reason may be reflected from one result of this study: PB processes at higher altitude tend to produce less frequent and smaller pulses. Fewer and smaller pulses make it difficult to trigger our system and to locate them. In fact, in many cases, we cannot determine the beginning of flashes at very high altitude.

As an example with relatively good location results, Figure 12 shows an IC flash initiated at 14.5 km. Even this flash only has one site (the closest) triggered continuously during the whole flash. *E*-change waveform at this site is shown in the figure. This flash starts with leader processes mainly propagating horizontally, presumably in the upper positive charge region. Later this leader continues propagating horizontally, while another leader starts to propagate downward. In the left plot, it is difficult to recognize any clear channels due to limited number of sources. *E*-change pulses before the red dashed line are all positive polarity. This flash would have been included in the 662 flash samples of this study, except the initial leader shows no clear upward propagation (section 2). This example is also consistent with the result that upward propagation speed decreases with increasing initiation altitude. We speculate that above certain altitude, initial leaders mainly propagate only horizontally. However, these initial leaders produce relatively few and small pulses, so detecting and locating them is difficult.

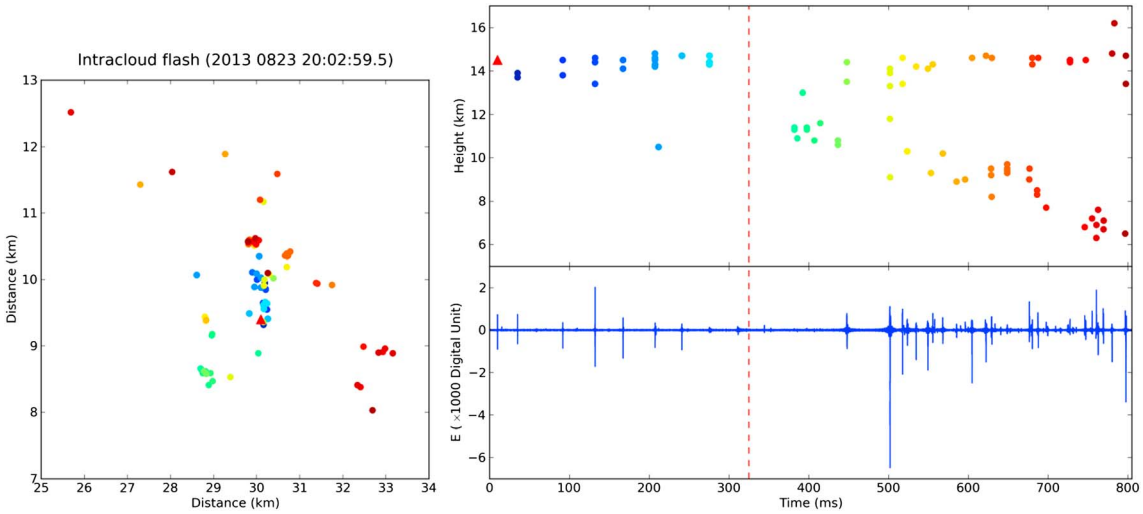


**Figure 12.** An IC flash initiated at a very high altitude (14.5 km). The red triangle represents the initial source of this flash. *E*-change pulses before the red dashed line are all positive polarity.

## 5. Conclusions

This study analyzed *E*-change records and 3-D locations of PB processes in 662 IC flashes. The large sample size enabled us to investigate possible associations among various characteristics of PB. The major conclusions of this study are summarized as follows.

The initiation altitude of PB in IC flashes predominantly lies in the 5 to 10 km range, with an average of 7.8 km. In comparison, PB in negative CG flashes lies between 4 and 7 km with an average of 5.7 km. Initial leaders during the PB stages in IC flashes are probably initiated between the main negative and upper positive charge regions and propagate upward. Initial leaders in negative CG flashes are probably initiated below the negative charge region and propagate downward.

Upward propagation speed of initial leaders during the PB stage in IC flashes ranges from 0.5 to $17.8 \times 10^5$ m/s with an average of $4.0 \times 10^5$ m/s. The speed clearly decreases with increasing initiation altitude.

Pulse rate, peak amplitude, and pulse width of PB pulses all show negative correlation with altitude and positive correlation with vertical speed. PB initiated at higher altitude tends to produce less frequent and smaller pulses with shorter pulse widths. The relationship between pulse rate and vertical speed has the strongest correlation, suggesting that each pulse in a PB pulse train probably corresponds to one step of the initial leader.

The average step length of each initial leader is estimated from pulse rate and vertical speed. The result shows that most of initial leaders have step length that ranged from 40 to 140 m with an average of 113 m. The step length has a strong connection with initiation altitude; leaders initiated at higher altitude tend to have longer steps.

The physical mechanisms behind the associations between different properties of PB are not fully understood. Longer steps at higher altitude are probably due to lower pressure and a longer mean free path of free electrons. PB pulse train characteristics including pulse rate, peak amplitude, and pulse width may be related with ambient electric field strength.

Because the upward propagation speed decreases with initiation altitude, it follows that flashes initiated high enough will have no vertical motion at all and only propagate horizontally. One such example is presented. The flash is initiated at an altitude of 14.5 km, and the initial leader propagates horizontally. There is also a train of positive pulses at the beginning of this flash, similar to a PB pulse train. However, because PB initiated at higher altitude tends to produce less frequent and smaller pulses, it is relatively difficult to detect and locate PB at very high altitude.

Future studies will analyze characteristics of PB in CG flashes and investigate whether its characteristics also vary with initiation altitude and propagation speed.

**Acknowledgments**
The data for this paper were obtained during the summer campaign in 2013. Readers can request the data from the corresponding author (wu.ting@comf5.comm.eng.osaka-u.ac.jp). This work was supported by Japanese Ministry of Education, Science, Sports and Culture, a Japanese Grant-in-Aid for Scientific Research.

## References

Baharudin, Z. A., N. A. Ahmad, M. Fernando, V. Cooray, and J. S. Makela (2012), Comparative study on preliminary breakdown pulse trains observed in Johor Malaysia and Florida, USA, *Atmos. Res.*, *117*, 111–121.

Bazelyan, E. M., and Y. P. Raizer (1998), *Spark Discharge*, Chem. Rubber Co., New York.

Behnke, S., R. Thomas, P. Krehbiel, and W. Rison (2005), Initial leader velocities during intracloud lightning: Possible evidence for a runaway breakdown effect, *J. Geophys. Res.*, *110*, D10207, doi:10.1029/2004JD005312.

Bitzer, P. M., H. J. Christian, M. Stewart, J. Burchfield, S. Podgorny, D. Corredor, J. Hall, E. Kuznetsov, and V. Franklin (2013), Characterization and applications of VLF/LF source locations from lightning using the Huntsville Alabama Marx Meter Array, *J. Geophys. Res. Atmos.*, *118*, 3120–3138, doi:10.1002/jgrd.50271.

Campos, L. Z. S., and M. M. F. Saba (2013), Visible channel development during the initial breakdown of a natural negative cloud-to-ground flash, *Geophys. Res. Lett.*, *40*, 4756–4761, doi:10.1002/grl.50904.

Edens, H. E., K. B. Eack, W. Rison, and S. J. Hunyady (2014), Photographic observations of streamers and steps in a cloud-to-air negative leader, *Geophys. Res. Lett.*, *41*, 1336–1342, doi:10.1002/2013GL059180.

Gomes, C., and V. Cooray (2004), Radiation field pulses associated with the initiation of positive cloud to ground lightning flashes, *J. Atmos. Sol. Terr. Phys.*, *66*(12), 1047–1055, doi:10.1016/j.jastp.2004.03.015.

Gomes, C., V. Cooray, and C. Jayaratne (1998), Comparison of preliminary breakdown pulses observed in Sweden and in Sri Lanka, *J. Atmos. Sol. Terr. Phys.*, *60*, 975–979, doi:10.1016/S1364-6826(98)00007-8.

Karunarathne, S., T. C. Marshall, M. Stolzenburg, N. Karunarathna, L. E. Vickers, T. A. Warner, and R. E. Orville (2013), Locating initial breakdown pulses using electric field change network, *J. Geophys. Res. Atmos.*, *118*, 7129–7141, doi:10.1002/jgrd.50441.

Krehbiel, P. R. (1986), The electrical structure of thunderstorms, in *The Earth's Electrical Environment*, pp. 90–113, National Academy Press, Washington, D. C.

Makela, J. S., N. Porjo, A. Makela, T. Tuomi, and V. Cooray (2008), Properties of preliminary breakdown processes in Scandinavian lightning, *J. Atmos. Sol. Terr. Phys.*, *70*(16), 2041–2052, doi:10.1016/j.jastp.2008.08.013.

Marshall, T., M. Stolzenburg, S. Karunarathne, S. Cummer, G. Lu, H.-D. Betz, M. Briggs, V. Connaughton, and S. Xiong (2013), Initial breakdown pulses in intracloud lightning flashes and their relation to terrestrial gamma ray flashes, *J. Geophys. Res. Atmos.*, *118*, 10,907–10,925, doi:10.1002/jgrd.50866.

Marshall, T., M. Stolzenburg, N. Karunarathna, and S. Karunarathne (2014), Electromagnetic activity before initial breakdown pulses of lightning, *J. Geophys. Res. Atmos.*, *119*, 12,558–12,574, doi:10.1002/2014JD022155.

Nag, A., and V. A. Rakov (2008), Pulse trains that are characteristic of preliminary breakdown in cloud-to-ground lightning but are not followed by return stroke pulses, *J. Geophys. Res.*, *113*, D01102, doi:10.1029/2007JD008489.

Petersen, D., and W. Beasley (2014), High-speed video observations of the preliminary breakdown phase of a negative cloud-to-ground lightning flash, paper presented at XV International Conference on Atmospheric Electricity, Norman, Okla., 15–20 June.

Rison, W., R. J. Thomas, P. R. Krehbiel, T. Hamlin, and J. Harlin (1999), A GPS-based three-dimensional lightning mapping system: Initial observations in central New Mexico, *J. Geophys. Res.*, *26*(23), 3573–3576, doi:10.1029/1999GL010856.

Shao, X. M., and P. R. Krehbiel (1996), The spatial and temporal development of intracloud lightning, *J. Geophys. Res.*, *101*(D21), 26,641–26,668, doi:10.1029/96JD01803.

Stolzenburg, M., W. D. Rust, and T. C. Marshall (1998), Electrical structure in thunderstorm convective regions: 3. Synthesis, *J. Geophys. Res.*, *103*(D12), 14,097–14,108, doi:10.1029/97JD03545.

Stolzenburg, M., T. C. Marshall, S. Karunarathne, N. Karunarathna, L. E. Vickers, T. A. Warner, R. E. Orville, and H.-D. Betz (2013), Luminosity of initial breakdown in lightning, *J. Geophys. Res. Atmos.*, *118*, 2918–2937, doi:10.1029/2012JD018675.

Stolzenburg, M., T. C. Marshall, S. Karunarathne, N. Karunarathna, and R. E. Orville (2014), Leader observations during the initial breakdown stage of a lightning flash, *J. Geophys. Res. Atmos.*, *119*, 12,198–12,221, doi:10.1002/2014JD021994.

Takahashi, T. (1978), Riming electrification as a charge generation mechanism in thunderstorms, *J. Atmos. Sci.*, *35*, 1536–1548, doi:10.1175/1520-0469(1978)035<1536:REAACG>2.0.CO;2.

Ushio, T., Z.-I. Kawasaki, K. Matsu-ura, and D. Wang (1998), Electric fields of initial breakdown in positive ground flash, *J. Geophys. Res.*, *103*(D12), 14,135–14,139, doi:10.1029/97JD01975.

Winn, W. P., G. D. Aulich, S. J. Hunyady, K. B. Eack, H. E. Edens, P. R. Krehbiel, W. Rison, and R. G. Sonnenfeld (2011), Lightning leader stepping, K changes, and other observations near an intracloud flash, *J. Geophys. Res.*, *116*, D23115, doi:10.1029/2011JD015998.

Wu, T., Y. Takayanagi, T. Funaki, S. Yoshida, T. Ushio, Z. Kawasaki, T. Morimoto, and M. Shimizu (2013), Preliminary breakdown pulses of cloud-to-ground lightning in winter thunderstorms in Japan, *J. Atmos. Sol. Terr. Phys.*, *102*, 91–98, doi:10.1016/j.jastp.2013.05.014.

Wu, T., S. Yoshida, T. Ushio, Z. Kawasaki, and D. Wang (2014), Lightning-initiator type of narrow bipolar events and their subsequent pulse trains, *J. Geophys. Res. Atmos.*, *119*, 7425–7438, doi:10.1002/2014JD021842.

Yoshida, S., T. Wu, T. Ushio, K. Kusunoki, and Y. Nakamura (2014), Initial results of LF sensor network for lightning observation and characteristics of lightning emission in LF band, *J. Geophys. Res. Atmos.*, *119*, 12,034–12,051, doi:10.1002/2014JD022065.

## Erratum

In the originally published version of this article, an error in the first key point was discovered. The error has since been corrected and this version may be considered the authoritative version of record.